

Differential Transverse Flow in Central C-Ne and C-Cu Collisions at 3.7 GeV/nucleon

L. Chkhaidze, T. Djobava*, L. Kharkhelauri

High Energy Physics Institute, Tbilisi State University

University St 9, 380086 Tbilisi, Republic of Georgia

Bao-An Li†

Department of Chemistry and Physics

P.O. Box 419, Arkansas State University

State University, Arkansas 72467-0419, USA

Differential transverse flow of protons and pions in central C-Ne and C-Cu collisions at a beam energy of 3.7 GeV/nucleon was measured as a function of transverse momentum at the SKM-200-GIBS setup of JINR. In agreement with predictions of a transversely moving thermal model, the strength of proton differential transverse flow is found to first increase gradually and then saturate with the increasing transverse momentum in both systems. While pions are preferentially emitted in the same direction of the proton transverse flow in the reaction of C-Ne, they exhibit an anti-flow to the opposite direction of the proton transverse flow in the reaction of C-Cu due to stronger shadowing effects of the heavier target in the whole range of transverse momentum.

PACS numbers: 25.70.-z; 25.75.Ld

*email: djobava@sun20.hepi.edu.ge

†email: Bali@astate.edu

I. INTRODUCTION

The ultimate goal of high energy heavy-ion studies is to investigate nuclear matter under extreme conditions of high density and temperature. In particular, extensive experimental and theoretical efforts have been devoted to probe the nuclear Equation of State (EOS), to identify the Quantum Chromodynamics (QCD) phase transition and to study properties of the Quark-Gluon Plasma (QGP) which is a novel form of matter. New information extracted from these studies is critical to many interesting questions in both nuclear physics and astrophysics. It is thus fundamentally important to find sensitive experimental probes of hot and dense nuclear matter. The collective phenomena found in heavy-ion collisions, such as the transverse (sideward directed) and elliptic flow of nuclear matter, have been shown to be among the most sensitive probes of the nuclear EOS. The transverse flow is the sideward deflection of nuclear matter moving forward and backward in the reaction plane. The transverse flow has been observed for nucleons, nuclear fragments and newly produced particles, such as pions and kaons, in heavy-ion collisions at all available energies ranging from the Fermi energy to the highest RHIC energy [1–6]. Especially, around 4 GeV/nucleon where a transition from “squeeze-out” perpendicular to the reaction plane to the in-plane flow is expected, a number of flow measurements have been carried out at the AGS/BNL [7,8] and the JINR/DUBNA [9–13]. Clear evidence of the transverse and elliptic flow effects for protons and π^- mesons have been obtained in central C-Ne and C-Cu collisions at energy of 3.7 GeV/nucleon by SKM-200-GIBS Collaboration at JINR/DUBNA. In C-Ne interactions the transverse flow of π^- mesons is in the same direction as for the protons, while in C-Cu collisions pions show antiflow behaviour. From the transverse momentum and azimuthal distributions of protons and π^- mesons with respect to the reaction plane defined by participant protons, the flow F (a measure of the collective transverse momentum transfer in the reaction plane) and the parameter a_2 (a measure of the anisotropic emission strength) have been extracted. The flow effects increase with the mass of the particle and the mass number of target A_T . The scaled flow $F_s = F/(A_P^{1/3} + A_T^{1/3})$ have been used for

comparison of transverse flow results of SKM-200-GIBS with flow data for various energies and projectile/target configurations. The F_s demonstrates a common scaling behaviour of protons flow values for different energies (Bevalac, GSI/SIS, Dubna, AGS, SPS) and systems. Focusing on the total transverse flow, i.e., integrated over transverse momentum, these studies have revealed much interesting physics. In the present work, we report results of a differential transverse flow analysis as a function of transverse momentum for protons and pions in central C-Ne and C-Cu collisions at a beam energy of 3.7 GeV/nucleon measured at the SKM-200-GIBS setup of JINR.

II. EXPERIMENT

The SKM-200-GIBS setup consists of a 2 m streamer chamber with volume $2 \times 1 \times 0.6 \text{ m}^3$, placed in a magnetic field of 0.8 Tesla, and a triggering system. The streamer chamber was exposed to a beam of C nuclei accelerated in the synchrotron up to a momentum of 4.5 GeV/c/nucleon (beam energy $E_{beam} = 3.7 \text{ GeV/nucleon}$). The thickness of the solid target Cu (in the form of a thin disc) was 0.2 g/cm^2 . Neon gas filling of the chamber also served as a nuclear target. Photographs of the events were taken using an optical system with three objectives. The experimental set-up and the logic of the triggering system are presented in Fig. 1.

The triggering system allowed the selection of “inelastic” and “central” collisions. The “inelastic” trigger, consisting of two sets of scintillation counters mounted upstream ($S_1 - S_4$) and downstream (S_5, S_6) the chamber, has been selecting all inelastic interactions of incident nuclei on a target. The “central” triggering system was consisting of the same upstream part as in the “inelastic” system and of scintillation veto counters (S_{ch}, S_n), registering a projectile and its charged and neutral spectator fragments, in the downstream part. All counters were made from the plastic scintillators and worked with photomultipliers PM-30. The S_1 counter with the scintillator of $20 \times 20 \times 0.5 \text{ cm}^3$ size, worked in the amplitude regime and identified the beam nuclei by the charge. The nuclei from the beam, going to the target, has been

selected using the profile counters S_2 , S_3 with the plastic of 15 mm diameter and 3 mm thickness and “thin” counter S_4 (15 mm and 0.1 mm correspondly). The S_{ch} counters (two counters with plastic of $25 \times 25 \times 0.5$ cm³ size) were placed at a distance of 6 m downstream the target and registered the secondary charged particles, emitted from the target within a cone of half angle $\Theta_{ch}=2.4^0$, 2.9^0 (the trigger efficiency was 99% for events with a single charged particle in the cone). The S_n counters registered the neutrons, emitted from the target in the solid angle $\Theta_n=1.8^0$, 2.8^0 (the trigger efficiency was 80% for one neutron). The S_n telescope consists from the five counters of $40 \times 40 \times 2$ cm³ size, layered by iron blocks of 10 cm thickness. The trigger selected central C-Ne and C-Cu collisions defined as those without charged projectile spectator fragments (with $p_Z > 3$ GeV/c) within a cone of half angle $\Theta_{ch} = 2.4^0$.

The streamer chamber pictures were scanned twice, and a subsequent third scan resolved ambiguities or discrepancies between two scans. Primary results of scanning and measurements were biased due to several experimental effects and appropriate corrections were introduced [14,15]:

- 1) The triggering system selected required projectile nuclei from a primary beam with an efficiency higher than 99%. The contamination due to interactions of other projectile nuclei with charge less than required biased the values of average multiplicities of secondary particles only insignificantly (the correction value $\leq 0.5\%$).
- 2) A trigger bias for central collisions arises whenever a projectile fragment hits the minimum bias veto-counter system and thus simulates a projectile-nucleus fragment. The effect was studied by simulating trajectories of secondary particles generated within the framework of the cascade model [16]. The geometry of the experimental set-up and magnetic field distribution were taken into account. The biases thus estimated turned out to be below statistical errors in multiplicity, p_t and y distributions.
- 3) The corrections due to secondary interactions within a solid target turned out to be negligible (the correction value $\leq 0.5\%$).
- 4) Pion detection was biased against low momenta. Pions were registered with practically

no bias when their momenta were $p \geq 40$ MeV/c for the solid targets and $p \geq 20$ MeV/c for gaseous Ne . Pions with lower momenta were also registered, however their detection efficiency depends on the path length in the target. The corrections could be delivered properly only for colliding with equal masses under the requirement of the symmetry $y - p_t$ plots in the c.m. system ($\sim 0.6\%$ in average multiplicity). A very rough estimation for asymmetric pairs of colliding nuclei showed that the correction values are $(0.5 - 2)\%$.

5) The samples of negative secondaries include K^- and Σ^- tracks. The contamination was estimated from pp data [17] and from our results on strange particle production [18] (the correction value $\leq 0.5\%$).

6) Corrections for scanning losses originate from two sources:

a) scanning inefficiency ($\sim 2\%$);

b) losses of the tracks with a small projection length (which may be screened by the target container or a flash around the vertex) and/or a small track curvature ($\sim 1 - 4\%$) The corrections were estimated under the requirement of azimuthal symmetry for each emission angle interval for all groups of the measured interactions separately. The correction values are $0.5 - 3.5\%$.

7) The measurement precision essentially depends on the track length and its dip angle. In the samples of events considered $\sim 5 - 15\%$ of π^- mesons turned out to be unmeasurable or were rejected because of large errors. The measurement losses of π^- mesons concerned practically only well determined intervals of emission angles, and, consequently, appropriate corrections, based on azimuthal symmetry, could be introduced in the spectra. Inaccuracy of the corrections was calculated, and systematic uncertainties of these corrections were found to be less than statistical ones. The ratio $\sigma_{cent}/\sigma_{inel}$ (that characterizes the centrality of selected events) is $(9\pm 1)\%$ for C-Ne and $(21\pm 3)\%$ for C-Cu. The average errors in measuring the momentum and production angle are $\langle \Delta p/p \rangle = (8-10)\%$ and $\Delta\Theta = 1^0 - 2^0$, respectively, for protons, while for pions $\langle \Delta p/p \rangle = 5\%$ and $\Delta\Theta = 0.5^0$, respectively.

III. DIFFERENTIAL FLOW OF NUCLEONS AND PIONS IN C-NE AND C-CU COLLISIONS

Several different methods have been utilized for analyzing flow effects in relativistic nuclear collisions, among them the transverse momentum analysis [19] and Fourier expansion of particle azimuthal angle distributions [20,21] have been most widely used. More recently, it has been found that the differential analysis of the flow strength as a function of transverse momentum is more useful in revealing detailed properties of the hot and dense matter, see, e.g. [6,22–25]. In this work, we adopt the method of differential flow analysis first used by the E877 collaboration in ref. [26]. Let $N^+(N^-)$ be the number of particles emitted in the same (opposite) direction of the transverse flow near projectile rapidity, then the ratio $R(p_t) = (dN^+/dp_t)/(dN^-/dp_t)$ as a function of p_t is a direct measure of the strength of differential flow near the projectile rapidity. It has been shown experimentally that more detailed information about the collective flow can be obtained by studying this ratio [26]. The differential flow data also provides a much more stringent test ground for relativistic heavy-ion reaction theories. It was shown theoretically by Li et al in ref. [27] and Voloshin in ref. [28] that the ratio $R(p_t)$ at high p_t is particularly useful in studying the EOS of dense and hot matter formed in relativistic heavy-ion collisions.

The data have been analysed event by event using the transverse momentum technique of P.Danielewicz and G.Odyniec [19]. The reaction plane have been defined for the participant protons i.e. protons which are not fragments of the projectile ($p/z > 3$ GeV/c , $\Theta < 4^0$) and target ($p/z < 0.2$ GeV/c). They represent the protons participating in the collision. The analysis have been carried out on 723 C-Ne and 663 events. The average multiplicities of participant protons are $\langle N_p \rangle = 12.4 \pm 0.5$ in C-Ne and $\langle N_p \rangle = 19.5 \pm 0.6$ in C-Cu, respectively.

The admixture of π^+ mesons amongst the protons is about (25÷27) %. For the event by event analysis it is necessary to perform an identification of π^+ mesons and separate them from the protons. The statistical method have been used for identification of π^+ mesons.

The main assumption is based on the similarity of spectra of π^- and π^+ mesons (n_π , p_t , p_l). The two-dimensional – transverse and longitudinal momentum distribution (p_t , p_l) have been used for identification of π^+ mesons. It had been assumed, that π^- and π^+ mesons hit a given cell of the plane (p_t , p_l) with equal probability. The difference in multiplicity of π^+ and π^- in each event was required to be no more than 2. After this procedure the admixture of π^+ is less than (5-7)%. The temperature of the identified protons agrees with our previous result [29], obtained by the spectra subtraction.

In the transverse momentum analysis technique of P.Danielewicz and G.Odyniec [19] the reaction plane is defined by the transverse vector \vec{Q}

$$\vec{Q} = \sum_{i=1}^n \omega_i \vec{p}_{\perp i} \quad (1)$$

where i is a particle index, ω_i is a weight and $p_{\perp i}$ is the transverse momentum of particle i . The reaction plane is the plane containing \vec{Q} and the beam axis. The weight ω_i is taken as 1 for $y_i > y_{cm}$ and -1 for $y_i < y_{cm}$, where y_{cm} is c.m.s. rapidity and y_i is the rapidity of particle i . Autocorrelations are removed by calculating \vec{Q} individually for each particle without including that particle into the sum (1).

$$\vec{Q}_j = \sum_{i \neq j}^n \omega_i \vec{p}_{\perp i} \quad (2)$$

The transverse momentum of each particle in the estimated reaction plane is calculated as

$$p_{xj}' = \frac{\sum_{i \neq j} \omega_i \cdot (\vec{p}_{\perp j} \cdot \vec{p}_{\perp i})}{|\vec{Q}_j|} \quad (3)$$

As we study an asymmetric pair of colliding nuclei, we chose to bypass the difficulties associated with the center-of-mass determination and carried out the analysis in the laboratory frame. We have replaced the original weight ω_i , by the continuous function $\omega_i = y_i - \langle y \rangle$ as in [30], where $\langle y \rangle$ is the average rapidity, calculated for each event over all the participant protons.

It is known [19], that the estimated reaction plane differs from the true one, due to the finite number of particles in each event. For the estimation of reaction plane resolution we

divided randomly each event into two equal sub-events (1 and 2) and the reaction plane vector in both half-events have been evaluated separately, getting \vec{Q}_1 and \vec{Q}_2 . Then estimated the azimuth angle difference between the vectors \vec{Q}_1 and \vec{Q}_2 $\Delta\varphi_R = \Phi_1 - \Phi_2$. The distributions of this $\Delta\varphi_R$ have been plotted for the whole experimental samples. The distributions are sharply peaked around $\Delta\varphi_R = 0$ (for C-Cu see Fig. 2). A uniform distributions have been recovered for the whole event (Φ) and two sub-events (Φ_1, Φ_2) reaction planes azimuth angles. According to ref. [19], the $\sigma_r \equiv \langle \Delta\varphi_R \rangle / 2$ is a good measure of the reaction plane resolution. We found that $\sigma_r = 26^\circ$ for C-Ne and $\sigma_r = 23^\circ$ for C-Cu, respectively.

First, in Fig. 3 we examine the transverse momentum spectra of protons detected on the same (dN^+/dp_t) and opposite (dN^-/dp_t) side of the transverse flow (reaction plane) in central C-Ne (window a) and C-Cu (window b) interactions, respectively. These protons are not used in the definition of the reaction plane. Here only protons emitted in the rapidity intervals of $1.7 < Y < 2.4$ for C-Ne and $1.3 < Y < 2.7$ for C-Cu, respectively, are considered. The chosen rapidity ranges are around the projectile rapidity of $Y_{proj} = 2.28$. In these rapidity ranges particles with high transverse momenta must have suffered very violent collisions and thus originate most likely from the very hot and dense participant region. On the other hand, particles with low transverse momenta are mostly from cold spectators. It is seen that there is a clear excess of protons emitted to the same side of the directed flow for both C-Ne and C-Cu collisions. In both collisions the spectra show typical exponential behaviour for $p_t \geq 0.2$ GeV/c. The spectra for particles in the same and opposite directions of the transverse flow are approximately parallel to each other at p_t larger than about 0.7 GeV/c. These findings are similar to those observed by the E877 collaboration for protons in central Au-Au collisions at a beam energy of 10.8 GeV/nucleon [26].

The above observations can be understood qualitatively within the transversely moving thermal model of Li et al. [27]. Assuming that all or a fraction of particles in a small rapidity bin around Y_{proj} are in local thermal equilibrium at a local temperature T , and the center of mass of these particles are moving with a velocity β along the transverse flow direction $+x$ in the reaction plane, then the transverse momentum spectrum of these particles can be

written as

$$\frac{d^3N}{p_t dp_t d\phi dY} = C \cdot \gamma(E - \beta \cdot p_t \cos(\phi)) \cdot e^{-\gamma(E - \beta p_t \cos(\phi))/T} \quad (4)$$

where C is a normalization constant, $\gamma = 1/\sqrt{1 - \beta^2}$ and ϕ is the azimuthal angle with respect to the reaction plane. The transverse momentum spectra for particles emitted in the same ($dN^+/p_t dp_t$) and opposite ($dN^-/p_t dp_t$) directions of the transverse flow are then

$$\frac{dN_{\pm}}{p_t dp_t} = C_{\pm} e^{-\gamma E/T} (\gamma E \mp T\alpha) e^{\pm\alpha} \quad (5)$$

where $\alpha \equiv \gamma\beta p_t/T$. These distributions reduce to simple exponents

$$\frac{dN_{\pm}}{p_t dp_t} \propto \exp(-p_t/T_{eff}^{\pm}) \quad (6)$$

at high transverse momenta p_t . In the above equation, the inverse slopes or effective temperatures T_{eff}^{\pm} in the semilogarithmic plot of the spectra at high p_t are

$$\frac{1}{T_{eff}^{\pm}} = - \lim_{p_t \rightarrow \infty} \left[\frac{d}{dp_t} \cdot \ln \left(\frac{dN^{\pm}}{p_t dp_t} \right) \right] = \frac{\gamma}{T} (\cosh(Y) \mp \beta). \quad (7)$$

In general, the inverse slope $1/T_{eff}^{\pm}$ reflects combined effects of the temperature T and the transverse flow velocity β . For the special case of considering particles at midrapidity, β is zero and the effective temperatures are equal to the local temperature T of the thermal source. Otherwise, one normally expects $T_{eff}^+ > T_{eff}^-$. For high energy heavy ion collisions in the region of 1 to 10 GeV/nucleon, β is much smaller than $\cosh(Y)$ around the projectile rapidity, thus one again expects $T_{eff}^+ \approx T_{eff}^-$ at high transverse momenta, i.e two approximately parallel spectra $dN^+/p_t dp_t$ and $dN^-/p_t dp_t$ at high p_t . The distributions (dN^+/dp_t) and (dN^-/dp_t) have been fitted by eq.(5). For C-Ne in the rapidity interval of $1.7 < Y < 2.4$ from the (dN^+/dp_t) spectra at high p_t ($p_t > 0.6$ GeV/c) the temperature T and flow velocity have been obtained: $T = 128 \pm 5$ MeV/c, $\beta = 0.016 \pm 0.004$; from the (dN^-/dp_t) spectra at high p_t the following values of temperature T and flow velocity have been obtained: $T = 130 \pm 4$ MeV/c, $\beta = 0.019 \pm 0.005$. For C-Cu in the rapidity interval of $1.3 < Y < 2.7$ respectively, from the (dN^+/dp_t) spectra at high p_t ($p_t > 0.6$ GeV/c): $T = 135 \pm 4$ MeV/c,

$\beta = 0.025 \pm 0.006$; from the (dN^-/dp_t) spectra: $T = 132 \pm 6$ MeV/c, $\beta = 0.023 \pm 0.007$. The results of fitting are superimposed on spectra in Fig. 3. One can see, that the values of temperatures and flow velocities from the (dN^+/dp_t) and (dN^-/dp_t) spectra coincide both for C-Ne and C-Cu.

To study the strength of differential transverse flow, we compare in Fig. 4 the ratios $R(p_t)$ as a function of p_t for C-Ne and C-Cu collisions. It is seen that the ratios increase gradually at low p_t and reach a limiting value of about 1.9 and 2.5 in the reaction of C-Ne and C-Cu, respectively. The values of $R(p_t)$ are greater than one in the whole transverse momentum range, indicating that protons are emitted preferentially in the flow direction at all transverse momenta. It is an unambiguous signature of the sideward collective flow. Similar results have also been obtained by the E877 collaboration for protons in Au-Au collisions at 10.8 GeV/nucleon where the ratio $R(p_t)$ increases with p_t and finally saturates at about 2.

The saturation of $R(p_t)$ at high p_t is also what one expects within the transversely moving thermal model. From Eq. 5 one obtains readily

$$R(p_t) = \frac{dN^+/p_t dp_t}{dN^-/p_t dp_t} = \frac{C_+}{C_-} \cdot \frac{1 - \beta \cdot \frac{p_t}{E}}{1 + \beta \cdot \frac{p_t}{E}} \cdot e^{2p_t \cdot \frac{\gamma\beta}{T}}. \quad (8)$$

This ratio normally increases with p_t for any given values of T and β , but it becomes almost a constant at high p_t for very small β/T ratios. In relativistic heavy-ion collisions, particles are emitted continuously at different freeze-out temperatures during the whole reaction process. In particular, particles with high p_t are mostly emitted in the early stage of the reaction from the most violent regions where the local temperatures are high. Since the ratio $R(p_t)$ varies very slowly with p_t for low β/T ratios, one thus expects an approximately constant value of $R(p_t)$ at high p_t . At low transverse momenta, however, $R(p_t)$ is affected mostly by particles from the cold spectators, and the ratio $R(p_t)$ approaches one as p_t goes to zero.

Now we turn to the analysis of differential transverse flow for negative pions in the C-Ne and C-Cu reactions. Shown in Fig. 5 are the $R(p_t)$ ratios for negative pions in the rapidity range of $1.0 < Y < 2.5$. The solid lines are the linear fits to the experimental data to

guide the eye. In the C-Ne collisions the ratio $R(p_t)$ is greater than one in the whole range of transverse momentum, indicating pions are flowing on average to the same direction as protons. Moreover, the strength of the pion differential transverse flow increases almost linearly with p_t and reaches about 1.2 at $p_t=0.9$ GeV/c. On the contrary, it is seen that an anti-flow is observed for π^- mesons in the reaction of C-Cu. Thus, in C-Ne interactions the pions are preferentially emitted in the direction of the proton transverse flow, while in C-Cu reactions pions are preferentially emitted away from the direction of the proton transverse flow. It is necessary to mention here that a similar target dependence of the pion preferential emission in asymmetric nucleus-nucleus collisions was first observed by the DIOGENE collaboration [31]. Our results are consistent with theirs. This target dependence of the apparent pion transverse flow was explained quantitatively by nuclear shadowing effects of the heavier target within nuclear transport models [32,33]. Our results on the pion differential transverse flow and its dependence on the target are thus also understandable.

IV. SUMMARY

In summary, the differential transverse flow of protons and pions in central C-Ne and C-Cu collisions at a beam energy of 3.7 GeV/nucleon were measured at the SKM-200-GIBS setup of JINR. The strength of proton differential transverse flow is found to first increase gradually and then saturate with the increasing transverse momentum. From the transverse momentum distributions of protons emitted in the reaction plane to the same and opposite side of the transverse flow the temperatures and flow velocity β have been extracted in C-Ne and C-Cu collisions. The observations are in qualitative agreement with predictions of a transversely moving thermal model. In the whole range of transverse momentum studied, pions are found to be preferentially emitted in the same direction of the proton transverse flow in the reaction of C-Ne, while an anti-flow of pions is found in the reaction of C-Cu due to stronger shadowing effects of the heavier target. The differential flow data for both protons and pions provide a more stringent testing ground for relativistic heavy-ion

reaction theories. Detailed comparisons with predictions of relativistic transport models on the differential flow will be useful to extract more reliable information about the nuclear EOS. Such an endeavor is underway and results will be published elsewhere.

V. ACKNOWLEDGEMENT

We would like to thank M. Anikina, A. Golokhvastov, S. Khorozov and J. Lukstins for fruitful collaboration during the obtaining of the data. The work of B.A. Li was supported in part by the U.S. National Science Foundation under Grant No. PHY-0088934 and the Arkansas Science and Technology Authority under Grant No. 00-B-14.

REFERENCES

- [1] G.D. Westfall, Nucl. Phys. **A630**, 27c (1998); *ibid*, **A681**, 343c (2001).
- [2] H.H. Gutbrod, A.M. Poskanzer and H.G. Ritter, Rep. Prog. Phys. **52**, 1267 (1989).
- [3] W. Reisdorf and H.G. Ritter, Ann. Rev. Nucl. Part. Sci. **47**, 663 (1997); N. Hermann, J.P. Wessels and T. Wienold, *ibid*, **49**, 581 (1999).
- [4] C.Ogilvie et.al., Nucl.Phys., **A638**, 57 (1998).
- [5] G. Rai, Nucl. Phys. **A681**, 181 (2001).
- [6] H.Appelshauser et. al.(NA49 collaboration), Phys. Rev. Lett., **80**, 4136 (1998); M.M.Aggarwal et. al., (WA98 collaboration), Phys. Lett. **B469**, 30 (1999); K.Ackermann et. al. (STAR collaboration), Phys. Rev. Lett., **86**, 402 (2001); K.Adcox et. al.(PHENIX Collaboration), Phys. Rev. Lett. **87**, 052301 (2001).
- [7] C. Pinkenburg et al. (E895 collaboration), Phys. Rev. Lett. **83**, 1295 (1999); H.Liu et.al.(E895 collaboration), *ibid*, **84**, 548 (2000).
- [8] B. Holzman et al (E917 Collaboration), nucl-ex/0103015, in QM01 Proc., Nucl., Phys. A (2001) in press.
- [9] L. Chkhaidze, T.Djobava et al., Phys. Lett., **B411**, 26 (1997).
- [10] L. Chkhaidze, T.Djobava et al., Phys. Lett., **B479**, 21 (2000).
- [11] Lj. Simic and J. Milosevic, J. Phys., **G27**, 183(2001).
- [12] B. Bannik et al., J. Phys., G14, 949 (1988).
- [13] M. Adamovich et al., Eur. Phys. J., **A6**, 427 (1999).
- [14] M. Anikina et al., JINR Dubna Report E1-84-785 (1984).
- [15] M. Anikina et al., Phys. Rev. **C33**, 895(1986).

- [16] K. Gudima, V. Toneev, Nucl. Phys. **A400**, 895(1983).
- [17] O. Benary, R. Price G. Alexander, UCRL -20000 NN report, 1970.
- [18] M. Anikina et al., Z. Phys. **C25**, 1(1984).
- [19] P. Danielewicz and G. Odyniec, Phys. Lett., **B157**, 146 (1985).
- [20] J.-Y. Ollitrault, Phys. Rev. **D46**, 229 (1992).
- [21] S. Voloshin and Y. Zhang, Z. Phys., **C70**, 665 (1996); A.M. Poskanzer and S.A. Voloshin, Phys. Rev., **C58**, 1671 (1998).
- [22] B.A. Li and A.T. Sustich, Phys. Rev. Lett. **82**, 5004 (1999); B.A. Li, *ibid*, **85**, 4224 (2000).
- [23] B.A. Li, A.T. Sustich and B. Zhang, nucl-th/0108047, Phys. Rev. **C64**, 054604 (2001).
- [24] M. Gyulassy, I. Vitev, X.-N. Wang, Phys. Rev. Lett. **86**, 2537 (2001).
- [25] A. Andronic et al. (FOPI Collaboration), Phys. Rev. **C64**, 041604 (2001).
- [26] J. Barrette et al. (E877 collaboration), Nucl. Phys. **A590**, 259c (1995).
- [27] B.A. Li, C.M. Ko and G.Q. Li, Phys. Rev. **C55**, 844(1996).
- [28] S.A. Voloshin, Phys. Rev. **C55**, R1630 (1997).
- [29] L. Chkhaidze al., Z. Phys. **C54**, 179(1992).
- [30] O. Beavis, Phys. Rev. **C45**, 299 (1992).
- [31] J. Gosset et al. (DIOGENE Collaboration), Phys. Rev. Lett., **62**, 1251 (1989); M. Demoulin et al. (DIOGENE Collaboration), Phys. Lett., **B241**, 476 (1990).
- [32] B.A. Li, W. Bauer and G.F. Bertsch, Phys. Rev., **C44**, 2095 (1991); B.A. Li, Nucl. Phys. **A570**, 797 (1994).
- [33] S.A. Bass, R. Mattiello, H. Stöcker, W. Greiner and C.Hartnack, Phys. Lett., **B302**,

381 (1994).

FIGURE CAPTIONS

Fig. 1. SKM-200-GIBS experimental set-up. The trigger and the trigger distances are not to scale.

Fig. 2. Reaction plane resolution for C-Cu collisions. The curve is the result of data approximation by the polynomial of 4-th order to guide the eye.

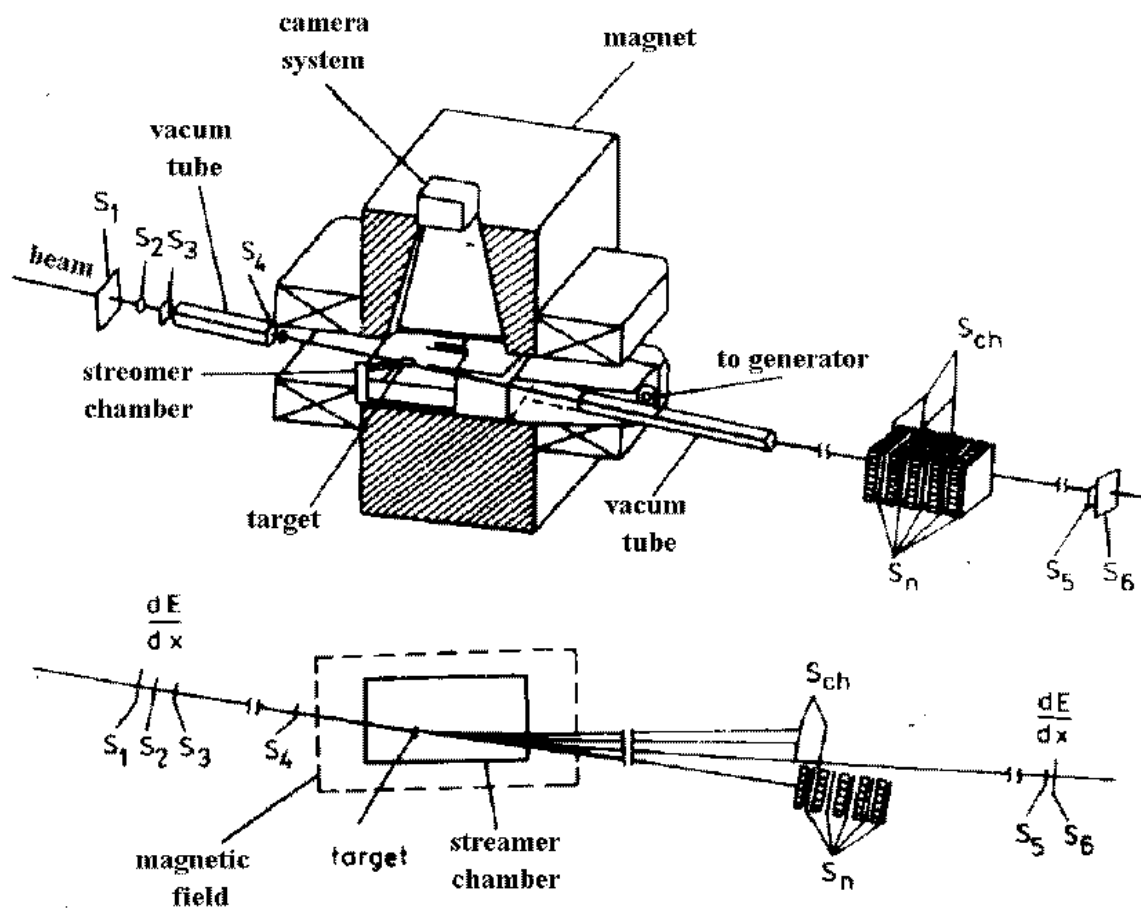
Fig. 3. The transverse momentum distributions of protons emitted in the reaction plane to the same (\circ) and opposite (Δ) side of the transverse flow in a) C-Ne and b) C-Cu collisions. The lines are results of fitting by eq.(5) at high p_t .

Fig. 4. Ratios of the yield of protons emitted to the same and opposite side of the transverse flow as a function of p_t in C-Ne (\circ) and C-Cu (Δ) collisions. The curves are logarithmic fits to guide the eye.

Fig. 5. Ratios of the yield of π^- mesons emitted to the same and opposite side of the transverse flow as a function of p_t in C-Ne (\circ) and C-Cu (Δ) collisions. The lines are linear fits to the data to guide the eye.

FIGURES

GIBS



"INELASTIC" TRIGGER = $S_1 \wedge S_2 \wedge S_3 \wedge S_4 \wedge \bar{S}_5 \wedge \bar{S}_6$

"CENTRAL" TRIGGER = $S_1 \wedge S_2 \wedge S_3 \wedge S_4 \wedge \bar{S}_n \wedge \bar{S}_{ch}$

FIG. 1. Experimental set-up. The trigger and trigger distances are not scale.

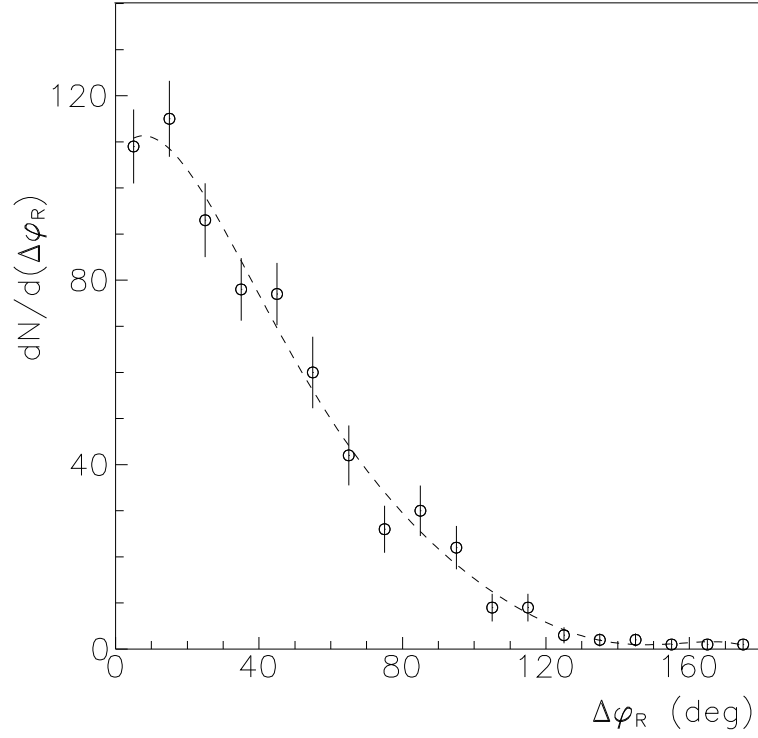


FIG. 2. Reaction plane resolution for C-Cu collisions. The curve is the result of data approximation by the polynomial of 4-th order to guide the eye.

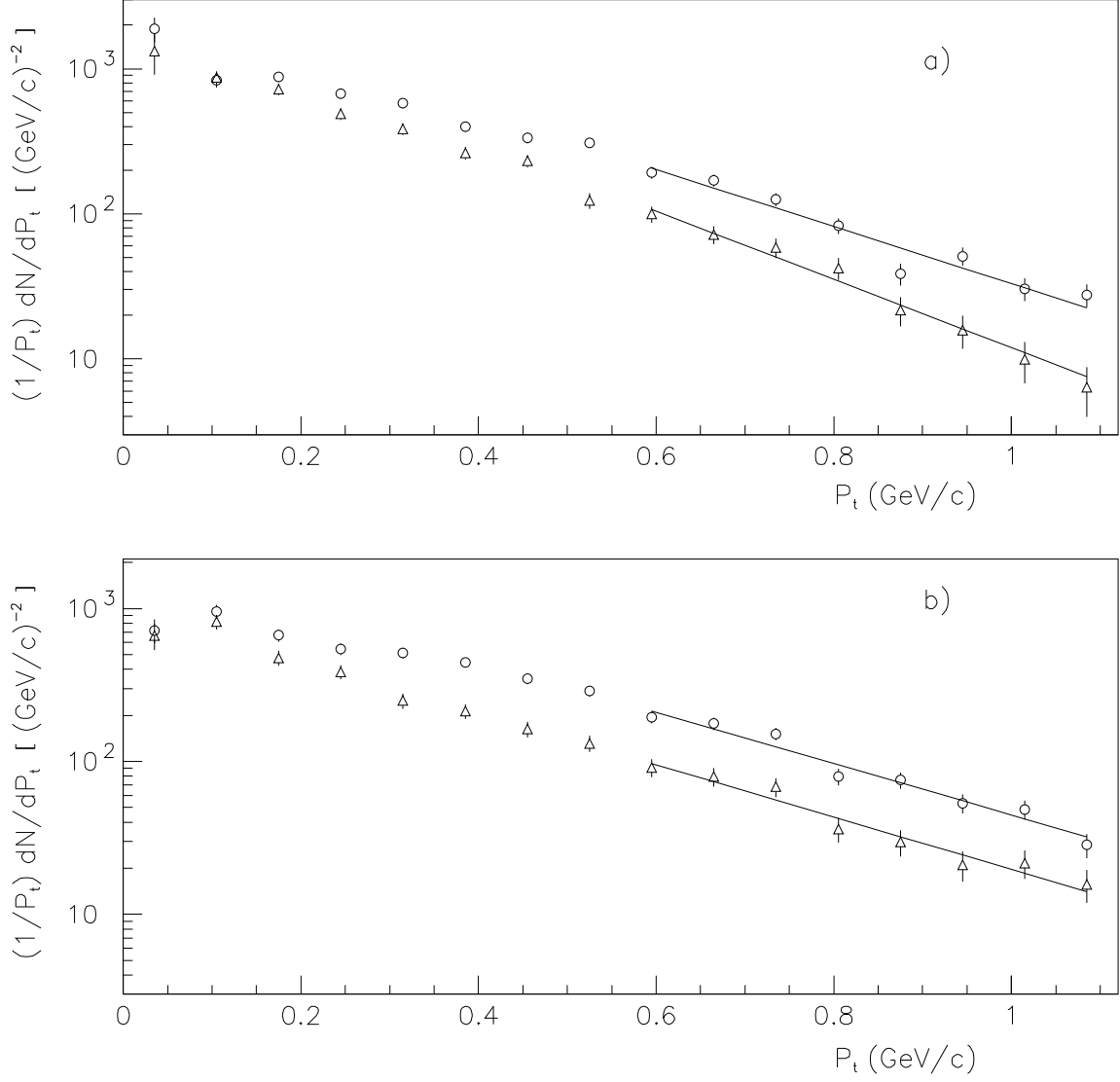


FIG. 3. The transverse momentum distributions of protons emitted in the reaction plane to the same (\circ) and opposite (\triangle) side of the transverse flow in a) C-Ne and b) C-Cu collisions. The lines are results of fitting by eq.(6) at high p_t .

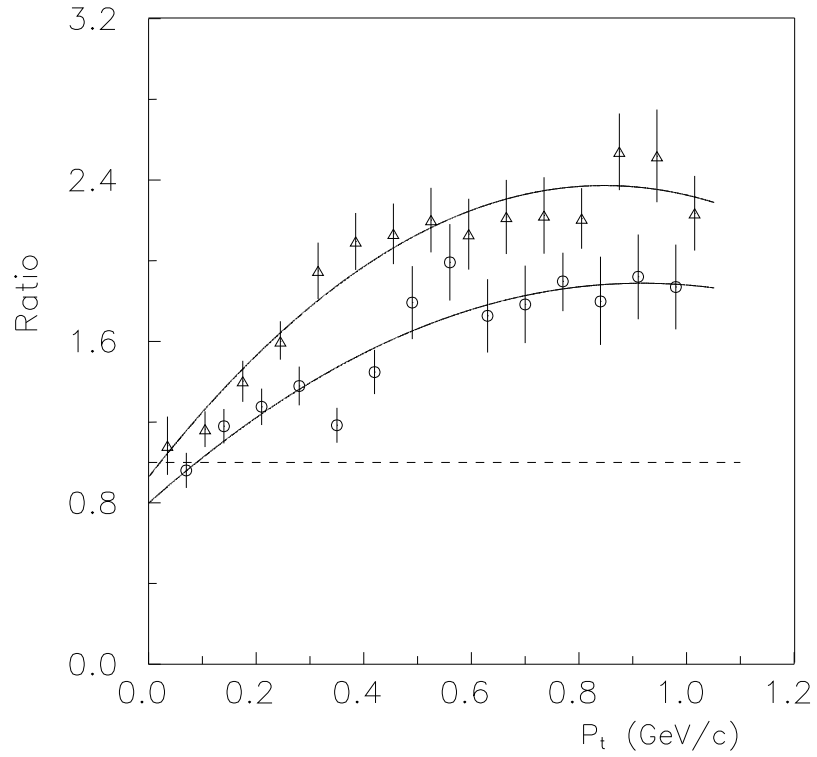


FIG. 4. Ratios of the yield of protons emitted to the same and opposite side of the transverse flow as a function of p_t in C-Ne (\circ) and C-Cu (\triangle) collisions. The curves are logarithmic fits to the data to guide the eye.

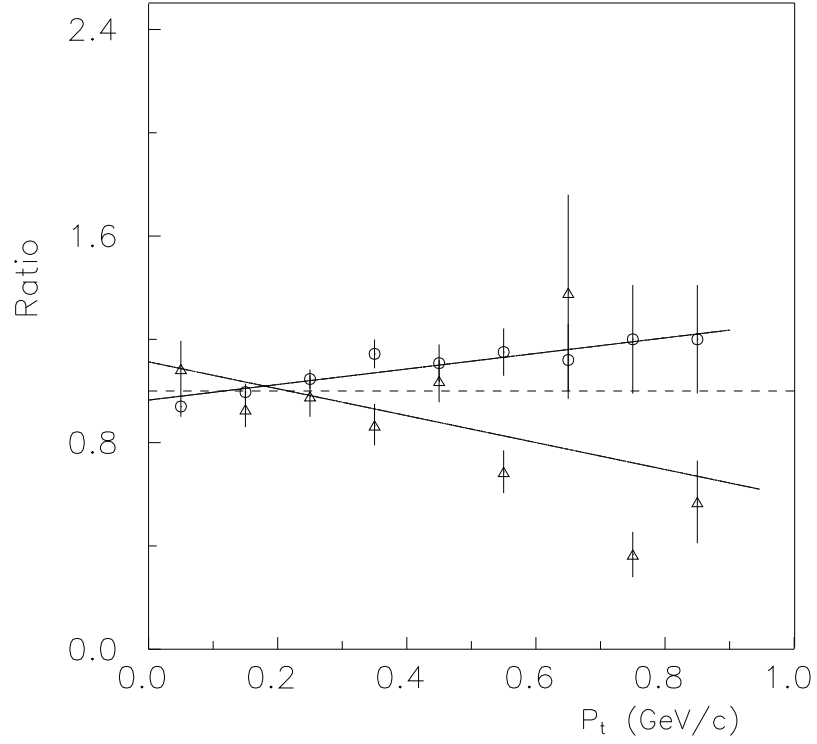


FIG. 5. Ratios of the yield of π^- mesons emitted to the same and opposite side of the transverse flow as a function of p_t in C-Ne (o) and C-Cu (Δ) collisions. The lines are linear fits to the data to guide the eye.